

Progress in Botany

Ulrich Lüttge
Wolfram Beyschlag
Burkhard Büdel
Dennis Francis
Editors

Progress in Botany 73

Genetics – Physiology
Systematics – Ecology

 Springer

Progress in Botany

Volume 73

Series Editors

Ulrich Lüttge, TU Darmstadt, Institut für Botanik,
FB Biologie (10), Schnittspahnstraße 3–5,
64287 Darmstadt, Germany

Wolfram Beyschlag, Fakultät für Biologie, Lehrstuhl für
Experimentelle Ökologie und Ökosystembiologie,
Universität Bielefeld, Universitätsstraße 25, 33615 Bielefeld,
Germany

Burkhard Büdel, TU Kaiserslautern,
FB Biologie, Abt. Allgemeine Botanik,
Erwin-Schrödinger-Str., 67663 Kaiserslautern,
Gebäude 13/2, Germany

Dennis Francis, University of Cardiff, Cardiff School
of Biosciences, Cardiff, United Kingdom CF10 3TL

Ulrich Lüttge • Wolfram Beyschlag •
Burkhard Büdel • Dennis Francis
Editors

Progress in Botany 73

 Springer

Editors

Prof. Dr. Ulrich Lüttge
TU Darmstadt
Inst. Botanik
Schnittspahnstr. 3–5
64287 Darmstadt
Germany
luettge@bio.tu-darmstadt.de

Prof. Dr. Burkhard Büdel
TU Kaiserslautern
FB Biologie
Abt. Allgemeine Botanik
Erwin-Schrödinger-Str.
67663 Kaiserslautern
Gebäude 13/2
Germany
buedel@rhrk.uni-kl.de

Prof. Dr. Wolfram Beyschlag
University of Bielefeld
Faculty of Biology
Experimental Ecology and
Ecosystem Biology
P.O. Box 10 01 31
33501 Bielefeld
Germany
w.beyschlag@uni-bielefeld.de

Dr. Dennis Francis
University of Cardiff
Cardiff School of Biosciences
Cardiff
United Kingdom
francisd@cardiff.ac.uk

ISSN 0340-4773

ISBN 978-3-642-22745-5 e-ISBN 978-3-642-22746-2

DOI 10.1007/978-3-642-22746-2

Springer Heidelberg Dordrecht London New York

Library of Congress Control Number: 33-15850

© Springer-Verlag Berlin Heidelberg 2012, Corrected printing 2012.

This work is subject to copyright. All rights are reserved, whether the whole or part of the material is concerned, specifically the rights of translation, reprinting, reuse of illustrations, recitation, broadcasting, reproduction on microfilm or in any other way, and storage in data banks. Duplication of this publication or parts thereof is permitted only under the provisions of the German Copyright Law of September 9, 1965, in its current version, and permission for use must always be obtained from Springer. Violations are liable to prosecution under the German Copyright Law.

The use of general descriptive names, registered names, trademarks, etc. in this publication does not imply, even in the absence of a specific statement, that such names are exempt from the relevant protective laws and regulations and therefore free for general use.

Printed on acid-free paper

Springer is part of Springer Science+Business Media (www.springer.com)

Series information

Progress in Botany is devoted to all the colourful aspects of plant biology. The annual volumes consist of invited reviews spanning the fields of molecular genetics, cell biology, physiology, comparative morphology, systematics, ecology, biotechnology and vegetation science, and combine the depth of the frontiers of research with considerable breadth of view. Thus, they establish unique links in a world of increasing specialization.

All chapters are thoroughly peer-reviewed by at least two independent referees.

Contents

Part I Review

A Half-Century Adventure in the Dynamics of Living Systems 3
Michel Thellier

Part II Genetics

**To Divide and to Rule; Regulating Cell Division in Roots
During Post-embryonic Growth** 57
Luis Sanz, James A.H. Murray and Walter Dewitte

**Metabolic Engineering of Cyanobacteria for Direct Conversion
of CO₂ to Hydrocarbon Biofuels** 81
Christer Jansson

Part III Physiology

**Interaction Between Salinity and Elevated CO₂:
A Physiological Approach** 97
Usue Pérez-López, Amaia Mena-Petite, and Alberto Muñoz-Rueda

**Mechanisms of Cd Hyperaccumulation and Detoxification
in Heavy Metal Hyperaccumulators: How Plants Cope with Cd** 127
Rong-Liang Qiu, Ye-Tao Tang, Xiao-Wen Zeng,
Palaniswamy Thangavel, Lu Tang, Yuan-Yuan Gan,
Rong-Rong Ying, and Shi-Zhong Wang

Long-Distance Transport and Plant Internal Cycling of N- and S-Compounds	161
Cornelia Herschbach, Arthur Gessler, and Heinz Rennenberg	
Blue-Light-Activated Chloroplast Movements: Progress in the Last Decade	189
Halina Gabryś	
Role of Chloroplast Thylakoid Lumen in Photosynthetic Regulation and Plant Cell Signaling	207
Cornelia Spetea	
Connecting Environmental Stimuli and Crassulacean Acid Metabolism Expression: Phytohormones and Other Signaling Molecules	231
Luciano Freschi and Helenice Mercier	
 Part IV Systematics	
Systematics of the Green Algae: A Brief Introduction to the Current Status	259
Thomas Friedl and Nataliya Rybalka	
 Part V Ecology	
Secondary Lichen Compounds as Protection Against Excess Solar Radiation and Herbivores	283
Knut Asbjørn Solhaug and Yngvar Gauslaa	
Index	305

Contributors

Walter Dewitte Cardiff School of Biosciences, University of Cardiff, Wales, UK, dewittew@cardiff.ac.uk

Luciano Freschi Department of Botany, Institute of Biosciences, University of São Paulo, CEP 05508-090 São Paulo, SP, Brazil

Thomas Friedl Experimental Phycology and Culture Collection of Algae (SAG), Georg August University Göttingen, Untere Karspüle 2a, 37073 Göttingen, Germany, tfriedl@uni-goettingen.de

Halina Gabryś Department of Plant Biotechnology, Jagiellonian University, Gronostajowa 7, 30-387 Kraków, Poland, halina.gabrys@uj.edu.pl

Yuan-Yuan Gan School of Environmental Science and Engineering, Sun Yat-sen University, Guangzhou 510275, People's Republic of China

Yngvar Gauslaa Department of Ecology and Natural Resource Management, Norwegian University of Life Sciences, P.O. Box 5003, 1432, Ås, Norway

Arthur Gessler Institute for Landscape Biogeochemistry, Leibnitz-Zentrum für Agrarlandschaftsforschung (ZALF) e.V, Eberswalderstr. 84, 15374 Müncheberg, Germany; Humboldt-University at Berlin, Lentze-Allee 75, 14195 Berlin, Germany

Cornelia Herschbach Institute of Forest Botany and Tree Physiology, Albert-Ludwigs-University Freiburg, Georges-Koehler Allee 53/54, 79085 Freiburg, Germany, cornelia.herschbach@ctp.uni-freiburg.de

Christer Jansson Lawrence Berkeley National Laboratory, Berkeley, CA 94720, USA, cgjansson@lbl.gov

Amaia Mena-Petite Departamento de Biología Vegetal y Ecología, Facultad de Ciencia y Tecnología, Universidad del PaísVasco/EHU, Apdo. 644, E-48080 Bilbao, Spain, amaia.mena@ehu.es

Helenice Mercier Department of Botany, Institute of Biosciences, University of São Paulo, CEP 05508-090 São Paulo, SP, Brazil, hmercier@usp.br

Alberto Muñoz-Rueda Departamento de Biología Vegetal y Ecología, Facultad de Ciencia y Tecnología, Universidad del PaísVasco/EHU, Apdo. 644, E-48080 Bilbao, Spain, a.munoz-rueda@ehu.es

James A.H. Murray Cardiff School of Biosciences, University of Cardiff, Wales, UK

Usue Pérez-López Departamento de Biología Vegetal y Ecología, Facultad de Ciencia y Tecnología, Universidad del PaísVasco/EHU, Apdo. 644, E-48080 Bilbao, Spain, usue.perez@ehu.es

Rong-Liang Qiu School of Environmental Science and Engineering, Sun Yat-sen University, Guangzhou 510275, People's Republic of China; Guangdong Provincial Key Lab of Environmental Pollution Control and Remediation Technology, Guangzhou 510275, People's Republic of China, eesqrl@mail.sysu.edu.cn

Heinz Rennenberg Institute of Forest Botany and Tree Physiology, Albert-Ludwigs-University Freiburg, Georges-Koehler Allee 53/54, 79085 Freiburg, Germany

Nataliya Rybalka Plant Cell Physiology and Biotechnology, Botanical Institute, Christian Albrechts University of Kiel, Am Botanischen Garten 1-9, 24118 Kiel, Germany, nrybalk@uni-goettingen.de

Luis Sanz Centro Hispano Luso de Investigaciones Agrarias, Universidad de Salamanca, Salamanca, Spain

Knut Asbjørn Solhaug Department of Ecology and Natural Resource Management, Norwegian University of Life Sciences, P.O. Box 5003, 1432, Ås, Norway, knut.solhaug@umb.no

Cornelia Spetea Department of Plant and Environmental Sciences, University of Gothenburg, PO Box 461, 405 30 Gothenburg, Sweden, cornelia.spetea.wiklund@dpes.gu.se

Lu Tang School of Environmental Science and Engineering, Sun Yat-sen University, Guangzhou 510275, People's Republic of China

Ye-Tao Tang School of Environmental Science and Engineering, Sun Yat-sen University, Guangzhou 510275, People's Republic of China; Guangdong Provincial Key Lab of Environmental Pollution Control and Remediation Technology, Guangzhou 510275, People's Republic of China

Palaniswamy Thangavel School of Environmental Science and Engineering, Sun Yat-sen University, Guangzhou 510275, People's Republic of China

Michel Thellier Laboratoire AMMIS, CNRS (DYCOEC: GDR 2984), Faculté des Sciences de l'Université de Rouen, 76821 Mont-Saint-Aignan Cedex, France, Michel.Thellier@univ-rouen.fr, michel.thellier0875@orange.fr

Shi-Zhong Wang School of Environmental Science and Engineering, Sun Yat-sen University, Guangzhou 510275, People's Republic of China; Guangdong Provincial Key Lab of Environmental Pollution Control and Remediation Technology, Guangzhou 510275, People's Republic of China

Rong-Rong Ying School of Environmental Science and Engineering, Sun Yat-sen University, Guangzhou 510275, People's Republic of China

Xiao-Wen Zeng School of Public Health, Sun Yat-sen University, Guangzhou 510080, People's Republic of China

Part I

Review

A Half-Century Adventure in the Dynamics of Living Systems

Michel Thellier

Contents

1	What is Life?	5
2	Methods and Methodological Improvements	5
2.1	Radioactive and Stable Tracers, the NCR and SIMS Techniques	5
2.2	Ionic Interactions, Ionic Condensation, Microelectrodes	7
2.3	Practical Applications	7
3	Enzyme-catalysed Reactions Under Non-classical conditions	9
3.1	Brief Reminder of Classical Enzyme Kinetics	9
3.2	Non-usual Cases of Enzyme Kinetics	10
3.3	Functioning-Dependent Structures	11
4	Fluxes of Solutes Exchanged by Biological Systems	14
4.1	Fluxes of Solutes Between Macroscopic Aqueous Compartments	14
4.2	Transport of Solutes by Plant Cells	17
5	Plant Sensitivity to Stimuli	24
5.1	Immediate and Local Responses in Separated Tissues or Cells	25
5.2	Migration, Storage and Recall of Information in Entire Plants	26
6	Reflection and Speculations	33
6.1	Methodological and Conceptual Implications	33
6.2	Physiological Considerations	34
7	Back to the Initial Question About Life	38
	Appendix	42
	References	51

Abstract In response to the question “What is life”, molecular biology has provided knowledge concerning the structure and function of the constituents of living systems. However, there still remains the point about understanding the dynamics of the processes involved in the functioning of the system. In our contribution to this quest, we began by some methodological improvements (especially

M. Thellier (✉)

Laboratoire AMMIS, CNRS (DYCOEC: GDR 2984), Faculté des Sciences de l’Université de Rouen, 76821 Mont-Saint-Aignan Cedex, France
e-mail: michel.thellier0875@orange.fr

concerning stable as well as radioactive isotopic tracers, ionic interactions and electrode measurements) and their possible applications to scientific or practical problems. Enzymatic reactions, fluxes of solutes and signalling processes play a crucial role in the dynamics of living systems. We have studied several non-usual cases of enzyme kinetics, particularly the functioning of those proteins that assemble when participating in a task and disassemble when the task is over (functioning-dependent structures or FDSs), and we have found that these FDSs could induce original regulatory properties in metabolic pathways. By studying fluxes of solutes through artificial (enzyme-grafted gel slabs) or real (frog skin) barriers, we have compared apparent kinetic parameters of the system with the real molecular parameters, and we have shown that increasing the complexity of a system may permit to evaluate parameters of the system that cannot be obtained using a conventional, reductionist approach. Concerning the transport of solutes between cells and their external medium, we have proposed to substitute a formalism derived from non-equilibrium thermodynamics for the classical combination of rectangular hyperbolas; in this interpretation, the important parameter is equivalent to a conductance; moreover we introduce a “symmetry-criterion” that is especially well adapted to discriminate active from passive exchanges between cells and exterior (while the Ussing’s flux ratio equation remains the easiest way to discriminate active from passive exchanges through an epithelium). Plants are sensitive to a number of stimuli, biotic or non-biotic, traumatic or non-traumatic. Simplified systems (such as foliar discs or cell suspension cultures) have permitted us to study some cell responses to stimuli. With entire plants, we show that migration, storage and recall of information can also take place, and that a plant can recall stored information several times. From all that, we come to the conclusion that an important characteristic of living beings is that not only the processes within them are dynamic but that even their structure is dynamic for a part.

Keywords Active vs. passive transports • Enzyme-grafted gel slabs • Enzyme kinetics • Flux-ratio equation • Functioning-dependent structures • Information recall • Information storage • Isotopic tracers • Plants • Solute fluxes • Stable isotopes • Symmetry-criterion

Abbreviations and Symbols

ACC	1-aminocyclopropane-1-carboxylic acid
FDS	Functioning-dependent structure
MAAC	Malonyl-1-aminocyclopropane-1-carboxylic acid
M–M	Michaelis–Menten
NCR	Neutron capture radiography
RCL function	The function enabling plants to recall stored information
SIMS	Secondary ion mass spectrometry
SPICE	Simulation programme with integrated circuit emphasis
STO function	The function permitting plants to store morphogenetic information

1 What is Life?

During centuries, a “vital strength” was assumed to have conferred on inanimate matter the property of becoming alive and of continuing to promote the spontaneous generation of living organisms from non-living material; however, not everyone agreed with this. The controversy continued to increase until the nineteenth century when all the experiments purporting to prove spontaneous generation were shown to be erroneous [see, for instance, Spallanzani (1787) and Pennetier (1907)]. Chemists succeeded in the abiotic synthesis of organic compounds (thus demonstrating that the substances produced by living processes and by artificial synthesis were not different in essence) and the theories of vitalism and spontaneous generation were abandoned.

Even before the old beliefs were rejected, a new approach, often termed “reductionism”, had begun to be developed. The aim was no longer to obtain a global interpretation of life, but to describe biological objects at the molecular, cytological and histological levels and to study how the structure of each object endowed it with its particular function. This resulted in the acquisition of fundamental biological knowledge and in the development of innovative agricultural, medical and industrial applications. However, it was also clear that the reductionist approach was not sufficient to give a fully satisfactory answer to the question “*What is life?*”

This answer entailed understanding not only the *function* but also the integrated *functioning* of biological objects. The availability of isotopic tracers, the increasing performance of computers and conceptual advances (e.g. the “*Catastrophe theory*” by René Thom, the “*Dissipative structures*” of Ilya Prigogine and the general theories of non-equilibrium thermodynamics and of dynamical systems) progressively provided researchers with scientific tools more efficient than those available to the physiologists of the previous centuries.

Our group has used these tools to address the problem of the nature of life [97, 108] in four complementary ways: (a) methodological improvements (and their practical applications), (b) kinetics of enzyme-catalysed reactions under unusual conditions (including the case of “functioning-dependent structures” and their role in cell regulation), (c) solute fluxes and transmembrane transports, (d) signalling and response to stimuli. We have used plants as experimental models in most cases. I have collaborated with many co-workers. Their contributions have always been valuable and sometimes essential. Their names appear in the list of our major publications, which rank in chronological order in the Appendix.

2 Methods and Methodological Improvements

2.1 *Radioactive and Stable Tracers, the NCR and SIMS Techniques*

My interest in the use of radioactive isotopes for autoradiography has been marginal [75], but I have made an extensive use of radioactive tracers for the measurement of

exchanges of inorganic ions and other solutes. The radioactive isotopes of a few elements of biological interest (such as Li, B, N and O) are, however, unusable because of their very short half-lives; but these elements have a stable isotope with a high cross-section for a nuclear reaction with thermal neutrons. The general expression of a nuclear reaction, $X(x, y)Y$, means that a radiation, x , interacts with a nuclide, X , to form another nuclide, Y , with the emission of one or several radiations, y . For the four isotopes under consideration, the nuclear reactions of interest are ${}^6\text{Li}(n, \alpha){}^3\text{H}$, ${}^{10}\text{B}(n, \alpha){}^7\text{Li}$, ${}^{14}\text{N}(n, p){}^{14}\text{C}$ and ${}^{17}\text{O}(n, \alpha){}^{14}\text{C}$, in which n is a thermal neutron, p a proton and α a helium (${}^4\text{He}$) nucleus. Following previous authors (Fick 1951; Hillert 1951; Faraggi et al. 1952), we have used these reactions for the imaging and the measurement of unidirectional fluxes of Li, B, N and O [1–2, 9, 12–13, 43–44, 58, 61, 67, 89]. The technique, which has been termed NCR for “Neutron-capture radiography” (Larsson et al. 1984), consists of sandwiching the sample between a quartz slide and a cellulose-nitrate film and irradiating the whole arrangement with thermal neutrons. When a radiation hits the film, it leaves a damage trail that can be enlarged by treatment with NaOH or KOH into a track visible by optical microscopy. The lateral resolution is of the order of a few micrometers; we have rendered the technique quantitative and we have contributed to show how to discriminate from one another the tracks originating from different nuclear reactions.

In the Secondary ion mass spectrometry (SIMS) method, which is also termed “Ionic analysis”, the specimen is bombarded by a narrow beam of ions (the “primary ions”) and the “secondary ions” that are sputtered from the specimen surface are collected, sorted by mass-spectrometry and arranged for building an image of the nuclide distribution at the specimen surface (Castaing and Slodzian 1962). Under the leadership of Camille Ripoll, the SIMS section of our laboratory was equipped initially with an IMS4F instrument [26, 55, 72, 80, 88, 120]. The machine was able to detect and image stable as well as radioactive isotopes of almost all chemical elements; several different secondary ions were detected quasi-simultaneously; the mass resolution allowed to discriminate secondary ions even when they were with the same mass number; the lateral resolution was of the order of 300 nm. In a collaboration with CAMECA (France) and Oxford Instruments (UK), our group has created a device permitting to study frozen-hydrated specimens [99, 113, 114], thus limiting the risk for mobile substances to be mobilised or lost during sample preparation. More recently, we have been equipped with a NanoSIMS50 instrument (Hillion et al. 1997) that can detect and image several different secondary ions strictly simultaneously with a lateral resolution of 50 nm.

For any system, the influx (or inflow), J_j^{ei} , of a solute, S_j , from exterior, e, to interior, i, is the unidirectional rate of S_j entry. An easy way to measure J_j^{ei} consists of labelling S_j in the external medium with a radioactive or a stable tracer, S_j^* , and measuring the progressive accumulation of S_j^* in the internal medium. Conversely, when an appropriate pre-treatment has permitted to label S_j with S_j^* in the internal medium, one may follow the outflux (or outflow), J_j^{ei} , of S_j (i.e. the unidirectional rate of S_j exit) by measuring the progressive accumulation of S_j^* in the external medium. The net flux (or net flow), J_j , of S_j is written

$$J_j = J_j^{\text{ei}} - J_j^{\text{ie}} \quad (1)$$

2.2 *Ionic Interactions, Ionic Condensation, Microelectrodes*

Inorganic ions (also termed “small ions”) interact with one another and with the non-mobile distributions of electric charges borne by macromolecules [73]. With Maurice Demarty [15, 21, 42, 82], we have studied the binding of small cations with the anionic sites existing in plant cell walls. We have determined capacities of calcium fixation, saturation kinetics, dissociation constants and ionic selectivities (e.g. $\text{Ca}^{2+}/\text{Na}^+$, $\text{Ca}^{2+}/\text{K}^+$ or Na^+/K^+). Using diffusion measurements in films made of isolated cell walls embedded in cellulose nitrate, we have also measured the mobility of the main cations (Na^+ , K^+ , Ca^{2+} , Mg^{2+}).

The inorganic cations present in living material are usually considered to be either free or bound; but this is an oversimplification, especially because it neglects the phenomenon of “ionic condensation” (Manning 1969, 1996). In the presence of polymers arranged in a linear distribution of non-mobile electric charges, some of the free counterions (ions with a sign opposite to that of the fixed charges) “condense” on the polymers at a critical value of the polymer charge density. This phenomenon resembles a phase transition. The condensed counterions are delocalised and can diffuse along the polymers, but they cannot leave their close vicinity. The divalent ions condense before the monovalent, the trivalent before the divalent, etc. Since the charge-density of the aligned polymers is easily increased or decreased (e.g. following the action of enzymes such as kinases and phosphatases), this can control the relative concentrations of free and condensed counterions; reciprocally, the calcium condensation/decondensation can change the activity of calcium-dependent kinases and phosphatases and consequently modulate the density of the non-mobile aligned charges. With Camille Ripoll, we have envisaged the possibility that these processes have a role in signal transduction [109].

With Jean-Paul Lassalles [47, 50, 52], we have determined sub-cellular electrical characteristics by use of microelectrodes and we have analysed the electrical noise to study transmembrane ion transports. The method was suited to the determination of vacuole ATPase activities, the electric resistance of cell membranes, the characteristics of passive ionic channels and the effect of introducing inorganic ions or pharmacological agents into the vacuole.

2.3 *Practical Applications*

Apart from using the above techniques for our own researches, we have been solicited by other teams for collaborations concerning diverse scientific or practical problems.

Using NCR, we have quantitatively imaged boron in plants at the tissue and cell levels for agronomical purpose [30, 57, 77, 83, 98, 106]. A part of this work was done in Costa Rica with the support of the “International Atomic Energy Agency”. In flax seedlings, boron concentrations were measured in the vacuoles and in the primary and secondary walls of cells in various tissues. In the foliar parenchyma of clover seedlings, boron was shown to come from seed reserves and root uptake in

approximate ratios of 50%/50% in the cytoplasm and 25%/75% in the cell walls; this suggests that apoplasmic migration occurs. After foliar application, in some plant species (e.g. clover) most of the boron remained immobilised at the site of application; in other species (e.g. young coffee trees), boron was rapidly distributed in the entire plant; this discrepancy was explained by differences in the plant content of sorbitol complexes (Brown et al. 1999). Boron was remobilized from old leaves to younger tissues [30].

In boron neutron capture therapy (a method for cancer treatment), ^{10}B -loaded molecules are accumulated in the tumour cells, which they kill thanks to the ionising particles produced by the $^{10}\text{B}(n,\alpha)^7\text{Li}$ nuclear reaction under neutron irradiation. Using NCR, we have measured ^{10}B contents in the tumour and in the neighbouring healthy cells [63, 87, 89, 104].

Lithium administration has specific effects such as treating some mental disorders or causing teratologic abnormalities. Using NCR [19–20, 24, 28, 36, 49, 65], we were the first to show that (a) lithium was finely regionalised in the brain of normal adult mice, whereas it was almost homogeneously distributed in the brain of foetuses or of adult demyelinating mutants, (b) Li equilibration between plasma and brain was very rapid, (c) in foetuses borne by Li-treated mice, lithium was concentrated in bones, heart, eyes and endocrine glands (which were also tissues sensitive to teratogenic Li effects) [46, 94] and (d) in cells, lithium seemed to accumulate close to the plasma membrane [81].

With SIMS, we have developed a method, based on the isotopic dilution $^6\text{Li}/^7\text{Li}$, for the determination of lithium concentrations in small liquid samples [60]. The same method can be extended to the determination of the concentration of any element possessing two stable isotopes or of any substance labelled with these isotopes. By combining the use of NCR and SIMS with that of a nuclear probe, we have contributed to show that the stable isotopes ^{14}N and ^{15}N can be used for the fine localisation and the labelling of nitrogen-containing substances, with a view to application to environmental, biological or agricultural projects [71, 74, 86, 92]. ^{15}N labelling was used for the study of NO pollution [102]. With the support of a doctoral fellowship for environment and energy control, we have used the stable isotopes ^{17}O and ^{18}O and their detection by NCR and SIMS for oxygen labelling, especially for the labelling of CO by ^{18}O in order to study the effect of CO pollution on pollen grains [100].

With our Australian Colleague Ross Jeffree, we have used SIMS for the depth profiling of manganese in shells of the bivalve *Hyridella* with a view to reconstitute the history of the pollutions by manganese rejects [91]. Again by SIMS depth profiling [69], we have determined ionic ratios in the cuticle of plant cells; by coupling the use of SIMS with a differential extraction of calcium and pectic substances in different wall areas [70], we have found that the binding of the pectic molecules with one another was mainly due to calcium bridges in the intercellular junctions of most cells and to covalent bonding in the internal part of the wall of the epidermal cells. Both types of bond were coexisting in the intercellular junctions of the cortical parenchyma.

In collaboration with Odile Morvan and with the support of a grant from the Technical Institute for Flax, we have shown that the differentiation of the secondary

walls of flax fibres was accompanied by a strong increase of the Na/Ca ratio [79]. In flax seeds [84], Ca and Mg were located within the protein bodies, Na was out of the protein bodies and K was scattered all over the seed tissues. With the support of a grant from the Ministry for teaching and research, we have observed a transient increase of calcium in beech cambium and phloem at the end of the period of quiescence [96].

With isolated cell walls of *Lemna* fronds, there was a high selectivity in favour of divalent vs. monovalent cations, whereas the selectivity between monovalent cations was always close to 1 [15]. In flax epidermal cell walls, calcium bridges bound galacturonic polysaccharides to one another [90]. Ionic condensation explained why the salt activity was low in the cell walls of plants adapted to saline habitats, in the presence of high external saline concentrations [25].

In brief. Radioactive tracers are commonly employed for imaging by autoradiography and for the determination of unidirectional fluxes of solutes by isotopic labelling. Here we show that techniques such as “Neutron capture radiography” and “Secondary ion mass spectrometry” enable one to use stable isotopes for imaging and labelling purposes with capabilities comparable to those with radioisotopes. Moreover, these techniques can be used in cases when the chemical elements under study do not possess any radioactive isotope with a half-life suited to tracer studies. Ionic interactions are omnipresent in living tissues. We have adapted classical physico-chemical techniques to the study of the interactions taking place between non-mobile charges (e.g. charges borne by macromolecules or cell organites) and small inorganic ions. The role of “Ionic condensation” should not be underestimated, though usually neglected by biologists. Subcellular characteristics have been determined by use of microelectrodes. Apart from using these techniques in our main studies, we have adapted them to a number of practical applications to agronomical, ecological and medical problems.

3 Enzyme-catalysed Reactions Under Non-classical conditions

3.1 Brief Reminder of Classical Enzyme Kinetics

In the case of Michaelis–Menten kinetics, each enzyme is monomeric and possesses a single catalytic site and no regulatory site. Under steady-state conditions and assuming a few simplifying hypotheses, the curve representing the reaction rate, v , as a function of the concentration, c_s , of the substrate, S , is a rectangular hyperbola

$$v = V_m \cdot c_s / (K_m + c_s) \quad (2)$$

V_m is the maximum rate of the reaction (enzyme saturated by the substrate), K_m is the “Michaelis constant” and $1/K_m$ corresponds approximately to the enzyme affinity for S . By contrast, allosteric enzymes (Monod et al. 1965) are polymeric and possess several catalytic sites and, possibly, one or several activatory or

inhibitory sites; assuming again a few simplifying hypotheses, the rate of functioning becomes a sigmoid function of c_s

$$v = V \cdot (c_s)^n / ((K)^n + (c_s)^n) \quad (3)$$

(Hill empirical equation) in which V , K and n are the parameters of the system. Due to the sigmoid form of the curve $\{c_s, v\}$, there is a narrow domain of c_s -values before and after which the enzyme activity is close to zero and quasi maximal, respectively. The binding of an activator (or of an inhibitor) displaces this threshold domain towards lower (or higher) c_s -values.

3.2 *Non-usual Cases of Enzyme Kinetics*

In cells, enzymatic reactions are often arranged in sequences, termed metabolic pathways, which transform an initial substrate into a final product through a series of intermediates. With Donald Mikulecky, we have studied a model sequence of four Michaelis–Menten enzymes followed by an allosteric enzyme. Using a simplified version of the SPICE programme (SPICE = Simulation programme with integrated circuit emphasis), we have calculated the time-courses of the concentrations of all the intermediates according to whether the initial substrate of the sequence was not or was an activator of the allosteric enzyme [78]. When the initial substrate is an activator, this is termed a feedforward control, a situation that occurs in the glycolytic pathway (Bali and Thomas 2001). In the feedforward case, a reversal of the direction of the reaction occurred before reaching equilibrium. The corresponding stationary states and their preceding transients were obtained by clamping the concentration of one intermediate. The same approach can be used for cases when a feedback control takes place or when oscillations or chaos occur.

Some enzymes can function in organic solvents (Butler 1979). We have studied the chymotrypsin-catalysed hydrolysis/synthesis of a peptide bond in mixtures of water and 1,4-butanediol, which is of the Michaelis–Menten type. Apparent parameters V_m^{app} and K_m^{app} were evaluated by adjusting a rectangular hyperbola to the experimental points $\{c_s, v\}$; real kinetic parameters, V_m and K_m were determined by taking into account the partition of the substrate between the catalytic site of the enzyme and the butanediol. Decreasing the water content from 100% to 20% caused the V_m^{app} -value to be reduced by a factor of 2 and the K_m^{app} -value to increase exponentially, while the V_m and K_m values were unchanged [76, 107].

When a Michaelis–Menten enzyme was immobilized in a gel slab bathing in aqueous solutions, different forms of $\{c_s, v\}$ curves (hyperbolic, sigmoid, dual-phasic, etc.) were observed, depending on the structural characteristics of the system (enzyme concentration within the gel, shape and dimensions of the gel phase, possible existence of pH gradients, etc.) [35]. In some cases, it was possible to adjust a combination of two rectangular hyperbolas to the experimental $\{c_s, v\}$

points, although a single enzyme was present. Even when a single rectangular hyperbola could be adjusted to the experimental points, the values of the apparent parameters, V_m^{app} and K_m^{app} , had no reason to be identical with the real enzymatic parameters, V_m and K_m .

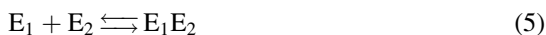
3.3 *Functioning-Dependent Structures*

Proteins involved in metabolic or signalling pathways often assemble into complexes ranging from quasi-static to transient dynamic associations (Sreer 1987; Ovadi 1988; Spirin and Mirny 2003). Hyperstructures represent a level of organisation intermediate between molecules and cells (Norris and Fishov 2001). At the interface between these two concepts [118, 121], we have introduced the notion of “Functioning-dependent structure” (FDS). An FDS is an assembly of proteins that associate with one another when performing a task but dissociate when the task is over [115]. Many different proteins are sometimes involved in those associations (Bobik 2006; Cheng et al. 2008); but two-enzyme complexes are observed in most cases. There are advantages inherent in such associations. Complexes of proteins often offer a better resistance to degradation by hydrolytic enzymes than free proteins do (Buchler et al. 2005). In an assembly of sequential enzymes, it is usually admitted (Sreer 1987; Ovadi 1991; Winkel 2004), though sometimes disputed (Cornish-Bowden 1991; Wu et al. 1991), that the product of an enzyme is channelled to the catalytic site of the next enzyme without being liberated into the cellular medium. This protects labile reactants from degradation and protects the cellular medium from being poisoned by toxic reactants.

We have wondered whether the kinetics of FDS functioning might endow them with original regulatory abilities. To explore quantitatively this possibility, we have studied numerically the steady-state kinetics of a model system of two sequential monomeric enzymes, E_1 and E_2 , according to whether they were free or associated in an FDS [115–116]. In this modelling, E_1 and E_2 possessed a single catalytic site, had no activator or inhibitor sites and catalysed reactions with a single substrate and a single product, i.e.



The reactions involved are listed in Table 1. To take into account that an FDS is formed only when the enzymes are active, that is when they are engaged in enzyme–substrate complexes, the direct binding of E_1 with E_2



did not exist in the reaction scheme. The system thus comprised 17 different chemical species (free substances and complexes) and 29 reactions. The reactions

Table 1 Reactions involved in the model of FDS under study

Reaction number	Reaction	Rate constants	Equilibrium constant
1	$E_1 + S_1 \rightleftharpoons E_1 S_1$	k_{1f}, k_{1r}	K_1
2	$E_1 + S_2 \rightleftharpoons E_1 S_2$	k_{2f}, k_{2r}	K_2
3	$E_2 + S_2 \rightleftharpoons E_2 S_2$	k_{3f}, k_{3r}	K_3
4	$E_2 + S_3 \rightleftharpoons E_2 S_3$	k_{4f}, k_{4r}	K_4
5	$E_1 S_1 + E_2 \rightleftharpoons E_1 S_1 E_2$	k_{5f}, k_{5r}	K_5
6	$E_1 S_2 + E_2 \rightleftharpoons E_1 S_2 E_2$	k_{6f}, k_{6r}	K_6
7	$E_2 S_2 + E_1 \rightleftharpoons E_1 E_2 S_2$	k_{7f}, k_{7r}	K_7
8	$E_2 S_3 + E_1 \rightleftharpoons E_1 E_2 S_3$	k_{8f}, k_{8r}	K_8
9	$E_1 S_1 \rightleftharpoons E_1 S_2$	k_{9f}, k_{9r}	K_9
10	$E_2 S_2 \rightleftharpoons E_2 S_3$	k_{10f}, k_{10r}	K_{10}
11	$E_1 S_1 E_2 \rightleftharpoons E_1 S_2 E_2$	k_{11f}, k_{11r}	K_{11}
12	$E_1 S_2 E_2 \rightleftharpoons E_1 E_2 S_2$	k_{12f}, k_{12r}	K_{12}
13	$E_1 E_2 S_2 \rightleftharpoons E_1 E_2 S_3$	k_{13f}, k_{13r}	K_{13}
14	$E_1 S_1 E_2 + S_2 \rightleftharpoons E_1 S_1 E_2 S_2$	k_{14f}, k_{14r}	K_{14}
15	$E_1 S_2 E_2 + S_2 \rightleftharpoons E_1 S_2 E_2 S_2$	k_{15f}, k_{15r}	K_{15}
16	$E_1 S_2 E_2 + S_3 \rightleftharpoons E_1 S_2 E_2 S_3$	k_{16f}, k_{16r}	K_{16}
17	$E_1 E_2 S_2 + S_1 \rightleftharpoons E_1 S_1 E_2 S_2$	k_{17f}, k_{17r}	K_{17}
18	$E_1 E_2 S_2 + S_2 \rightleftharpoons E_1 S_2 E_2 S_2$	k_{18f}, k_{18r}	K_{18}
19	$E_1 S_1 E_2 + S_3 \rightleftharpoons E_1 S_1 E_2 S_3$	k_{19f}, k_{19r}	K_{19}
20	$E_1 E_2 S_3 + S_1 \rightleftharpoons E_1 S_1 E_2 S_3$	k_{20f}, k_{20r}	K_{20}
21	$E_1 E_2 S_3 + S_2 \rightleftharpoons E_1 S_2 E_2 S_3$	k_{21f}, k_{21r}	K_{21}
22	$E_1 S_1 + E_2 S_2 \rightleftharpoons E_1 S_1 E_2 S_2$	k_{22f}, k_{22r}	K_{22}
23	$E_1 S_1 + E_2 S_3 \rightleftharpoons E_1 S_1 E_2 S_3$	k_{23f}, k_{23r}	K_{23}
24	$E_1 S_2 + E_2 S_2 \rightleftharpoons E_1 S_2 E_2 S_2$	k_{24f}, k_{24r}	K_{24}
25	$E_1 S_2 + E_2 S_3 \rightleftharpoons E_1 S_2 E_2 S_3$	k_{25f}, k_{25r}	K_{25}
26	$E_1 S_1 E_2 S_2 \rightleftharpoons E_1 S_2 E_2 S_2$	k_{26f}, k_{26r}	K_{26}
27	$E_1 S_1 E_2 S_2 \rightleftharpoons E_1 S_2 E_2 S_3$	k_{27f}, k_{27r}	K_{27}
28	$E_1 S_2 E_2 S_2 \rightleftharpoons E_1 S_2 E_2 S_3$	k_{28f}, k_{28r}	K_{28}
29	$E_1 S_1 E_2 S_3 \rightleftharpoons E_1 S_2 E_2 S_3$	k_{29f}, k_{29r}	K_{29}
Global	$S_1 \rightleftharpoons S_3$	—	K

were characterised by their forward and reverse rate constants, k_{jf} and k_{jr} , and by their equilibrium constant, K_j , with

$$K_j = k_{jf}/k_{jr} \quad (6)$$

For easier analysis, the parameters and variable were expressed as dimensionless quantities. The definition of the dimensionless quantities imposed the relation

$$k_{1r} \equiv 1 \quad (7)$$

The equations of the system were obtained by writing down that (a) the total concentration of each enzyme, E_1 and E_2 , was constant and (b) the variation of the concentration of each chemical species was given by the balance of the reactions

producing and consuming that species. Whatever the pathway from S_1 to S_3 , the equilibrium constant, K , of the global reaction



kept obviously the same value. This imposed the existence of relationships between the rate constants. Among the 58 rate constants of the system (Table 1), only 43 were independent and could be given an arbitrary value in the numerical calculations. The 15 other rate constants had to be calculated. We have chosen the set of constants

$$K_1, K_2, K_3, K_5, K_9, K_{10}, K_{11}, K_{12}, K_{13}, K_{15}, K_{17}, K_{27}, K_{29}, K \text{ and } k_{1r} \text{ to } k_{29r} \quad (9)$$

as our base of independent parameters. Under steady-state conditions of functioning, external mechanisms were assumed to maintain S_1 and S_3 at a constant and zero concentration, respectively; the concentrations of the other species had ceased to vary.

The numerical simulation consisted in varying systematically the values allocated to the independent parameters, calculating the corresponding values of the non-independent parameters and solving the equations of the system. For each set of parameter values, a curve $\{s_1, v\}$ (in which v was the dimensionless, steady-state rate of functioning and s_1 was the dimensionless concentration of S_1) was drawn in a few minutes. Testing three values (low, middle and high) for each independent parameter would have represented a total of approximately 10^{20} different cases to be numerically simulated. We used our intuition to limit the numerical simulations to a reasonable number. We have found sets of parameter values such that the $\{s_1, v\}$ curves obtained with an FDS presented extended linear or invariant parts, or were with a v -value appreciably above zero only in a limited domain of s_1 -values (spike responses), or else exhibited step-like (sigmoid) or inverse-step responses [115]. In some cases, $\{s_1, v\}$ curves with two inflexion points, which conferred on them a “dual-phasic” aspect, were also observed; although their functional advantage is not clear, it is noteworthy that dual-phasic curves are often exhibited by both natural and artificial enzyme and transport systems (Sects. 3.2, 4.1.1 and 4.2.1).

Free enzymes also can generate linear and invariant responses [116] and the step responses are usually not as good as those obtained with allosteric enzymes (Sect. 3.1); but the spike and inverse-step responses complete nicely the panoply of regulatory functions that might exist in a metabolic pathway.

***In brief.** Among the quasi-infinite number of chemical reactions potentially existing in a cell, only those catalysed by enzymes proceed at a rate compatible with life. A considerable number of investigations have thus been devoted by many authors to study the kinetics of enzyme-catalysed reactions: in the simplest case (enzymes of the “Michaelis–Menten” [M–M] type studied in diluted solutions in vitro), the kinetic curves have the shape of a rectangular hyperbola characterised by two parameters, V_m and K_m ; in more complicated case (e.g. allosteric*

enzymes) the curve may become sigmoid, etc. Here, we have studied a few cases in which an enzyme was studied under more or less complex conditions. When an allosteric enzyme, inserted in a sequence of enzymes of the $M-M$ type, was subjected to feedforward control (activation by a substrate found earlier in the sequence), a reversal of the direction of the reaction occurred before reaching equilibrium and the sequence behaved as an “anticipatory system”. With enzymes of the $M-M$ type studied in a partly aqueous/partly organic solution or under organised conditions, apparent parameters, V_m^{app} and K_m^{app} , could be determined by adjusting one or several rectangular hyperbolas to the kinetic data, but these apparent parameters were not equal to the real kinetic parameters, V_m and K_m ; the number of hyperbolas adjusted to each kinetic curve was not representative of the number of enzymes involved; the existence of a sigmoid kinetic curve was not proof that an allosteric enzyme was present. The dynamic association of two sequential enzymes (Functioning-dependent structure [FDS]) occurring in an active metabolic pathway generated steady-state kinetics exhibiting the full range of basic input/output characteristics found in electronic circuits such as linearity, invariance, or the production of spike-, step- or inverse step-responses.

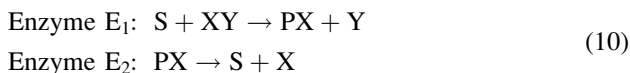
4 Fluxes of Solutes Exchanged by Biological Systems

4.1 Fluxes of Solutes Between Macroscopic Aqueous Compartments

In these experiments, an interface was separating two aqueous compartments, e and i (for exterior and interior). The compartments were large enough to allow the sampling of droplets for chemical analysis and the measurement of electric parameters.

4.1.1 Fluxes of Solutes Through an Enzyme-Grafted Gel Slab

Continuing the investigation described in the third paragraph of Sect. 3.2, we have examined a case [35] in which two enzymes of the Michaelis–Menten type, E_1 and E_2 , inserted at random in a gel slab separating compartments e and i, were catalysing reactions such as



At the start of the experiment, both compartments, e and i, contained equal concentrations of each solute (S, X, Y, XY and PX). The pH values in the

compartments were such that E_1 and E_2 were active only in layers of the gel slab, L_1 and L_2 , facing e and i , respectively. As a consequence of the concentration profiles thus created in the gel slab, an uphill transport of S occurred from e to i at the expense of the energy provided by the splitting of XY . This mimicked a first-order active transport in Mitchell's classification (Mitchell 1967). Depending on the structural features of the system (pH difference between e and i , enzyme concentrations in the gel slab, thicknesses of L_1 , L_2 and the inactive layer between them), the curve representing the rate, v , of the transport of S as a function of the concentration, c_s^e , of S in e exhibited a variety of shapes (e.g. hyperbolic, dual- or multi-phasic, sigmoid); moreover, when a combination of two rectangular hyperbolas could be adjusted to the experimental points $\{c_s^e, v\}$, no simple relationship was found to exist between the apparent parameters ($V_{m1}^{app}, K_{m1}^{app}, V_{m2}^{app}, K_{m2}^{app}$) calculated from the hyperbolas and the real parameters ($V_{m1}, K_{m1}, V_{m2}, K_{m2}$) of E_1 and E_2 .

In another investigation [56, 59], a single enzyme subjected to appropriate structural constraints catalysed an uphill transport of a solute, S_j , driven by a pH gradient. This was equivalent to a second-order active transport (Mitchell 1967). In that case, again the apparent kinetic parameters of the transport were generally not representative of the real kinetic parameters of the enzyme involved in this system.

4.1.2 Fluxes of Solutes Through an Isolated Frog Skin

4.1.2.1 Ussing's Flux-Ratio Equation

The ionic concentration of the fresh water in which frogs bathe is much less than that of their internal medium. Therefore, they tend to lose salt by diffusion. Maintaining their homeostasis requires the operation of an active, inward pumping of ions. Using metabolic inhibitors is not sufficient to determine which ion(s) is/are actively pumped, because the inhibitor may give rise to secondary effects altering also the transport of passively exchanged ions. Ussing (1949, 1971) mounted isolated frog skins between two aqueous compartments, e (on the external side of the skin) and i (on the internal side), and he proposed to discriminate the ions passively and actively exchanged by use of a "flux-ratio equation". If S_j is an ion exchanged between e and i , verifying

$$R \cdot T \cdot \ln\left(J_j^{ei}/J_j^{ie}\right) = R \cdot T \cdot \ln\left(c_j^e/c_j^i\right) - z_j \cdot F \cdot (\Psi^i - \Psi^e) \quad (11)$$

means that S_j is passively transported. In (11), R , T and F have their usual thermodynamic signification, J_j^{ei} and J_j^{ie} are the inflow and outflow of S_j , c_j^e and c_j^i are the external and internal concentrations of S_j , z_j is the electric charge of S_j and Ψ^e and Ψ^i are the external and internal electric potentials). By contrast, when

$$R \cdot T \cdot \ln\left(J_j^{ei}/J_j^{ie}\right) > R \cdot T \cdot \ln\left(c_j^e/c_j^i\right) - z_j \cdot F \cdot (\Psi^i - \Psi^e) \quad (12)$$

or

$$R \cdot T \cdot \ln\left(\frac{J_j^{ei}}{J_j^{ie}}\right) < R \cdot T \cdot \ln\left(\frac{c_j^e}{c_j^i}\right) - z_j \cdot F \cdot (\Psi^i - \Psi^e) \quad (13)$$

this means that S_j is actively transported from e to i or i to e, respectively.

When samples of frog skin were mounted between Ringer's solutions, sodium was actively pumped inwards (relationship (12) satisfied with $S_j = \text{Na}^+$). Under short-circuiting conditions (i.e. imposing $\Psi^i - \Psi^e = 0$), the net flux of sodium expressed in μA , J_{Na} (1), was equal to the electric intensity measured through the skin. This was meaning that sodium was the only ion for which the distribution was dependent on an active pumping; all the other ions were passively distributed. The ionic pump was subsequently shown to be a Mg-dependent Na^+-K^+ -ATPase, an enzyme that pumps Na^+ inwards and K^+ outwards (K^+ being immediately re-equilibrated between i and e by diffusion).

4.1.2.2 Lithium-Induced Electric Oscillations

Li^+ is the only ion that can replace Na^+ in the functioning of the ionic pump (Nagel 1977). In Ussing's experiments, the electric potential difference, ($\Psi^i - \Psi^e$), was stable; but, if lithium was partially or totally substituted for sodium in compartment e, ($\Psi^i - \Psi^e$) often became oscillatory (Takenaka 1936; Teorell 1954).

After studying the Li-induced oscillation experimentally [29], we modelled the skin epithelium [33] by two adjacent compartments, C_1 and C_2 , and three interfaces, a (between the external medium and C_1), b (between C_1 and C_2) and c (between C_2 and the internal medium). Interface a was considered a membrane permeable to Na^+ and Li^+ but almost impermeable to K^+ , interface b as a membrane bearing ATPases that pump Na^+ (or Li^+) from C_1 to C_2 and K^+ from C_2 to C_1 , and interface c as a diffusive barrier. In the numerical simulation of the model, we were able to render it consistent with the experimental observations only when a certain number of properties were fulfilled. The first of this property was

$$V_1/V_2 \ll 1 \quad (14)$$

in which V_1 and V_2 are the volumes of C_1 and C_2 per unit surface area of epithelium. This means that C_1 has to be much smaller than C_2 , thus excluding the possibility for C_1 and C_2 to correspond to the bulk of the cytoplasmic volume and to a few endoplasmic cisternae; C_1 was rather corresponding to cytoplasmic vacuoles transporting Na^+ or Li^+ ions and C_2 to intercellular spaces (most of the cell cytoplasm not being involved in Na^+ and Li^+ transport). Another requirement was

$$0 < \tau_1/\tau_2 < 1, \quad \text{with } 1 \text{ min} \leq \tau_1 \leq 5 \text{ min} \quad (15)$$

in which τ_1 and τ_2 are characteristic times corresponding to modifications of Li^+ in C_1 and K^+ in C_2 , respectively. If ρ and μ represent the ratio of the active vs. the passive fluxes of Li^+ and K^+ , respectively, the relationships

$$\rho \gg 1, \mu \gg 1, \quad \text{with } \rho \leq \mu \leq 2\rho \quad (16)$$

must also be satisfied, which means that ρ and μ have to be of the same order of magnitude. Finally, if P holds for the permeability coefficients of interfaces a, b and c for the ions Li^+ and K^+ , these coefficients have to obey the relationships

$$P_{\text{Li}^+}^a/P_{\text{K}^+}^c \ll 1, P_{\text{K}^+}^b/P_{\text{K}^+}^c \ll 1 \quad (17)$$

By inducing an oscillatory behaviour (as a consequence of adding lithium in the external medium) ,we have thus yielded information on the values of a few variables ($V_1, V_2, \tau_1, \tau_2, \rho, \mu, P_{\text{Li}^+}^a, P_{\text{K}^+}^b$ and $P_{\text{K}^+}^c$) that are characteristic of the system behaviour under natural conditions.

4.2 Transport of Solutes by Plant Cells

We term ‘‘cell transport’’, ‘‘transmembrane transport’’ or simply ‘‘transport’’ the exchange of solutes that takes place between the cells of entire plants or of separated tissues and their external medium. Solute transport must be distinguished from solute ‘‘migration’’, which corresponds to a movement of solutes at a lesser or greater distance within the plant. We term ‘‘carrier’’ any protein or assembly of proteins that catalyses the transmembrane transport of a solute. We have chosen cell suspension cultures or small aquatic plants as experimental models, because their exchanges of solutes were corresponding essentially to cell transport, while further solute migration was nil or extremely limited. We have revisited the conventional formulation of cell transport in order to get a Flow/Force description of the uptake of solutes.

4.2.1 Conventional Formulation of Cell Transport

The conventional formulation of cell transport was created for interpreting experimental measurements of the inflow, J_j^{ei} , of a solute S_j into a plant sample (e.g. a root system) as a function of the external concentration, c_j^{e} , of S_j . With a narrow range of c_j^{e} values, under steady-state conditions the distribution of points $\{c_j^{\text{e}}, J_j^{\text{ei}}\}$ often increases monotonically up to a plateau. Following a suggestion by Emmanuel Epstein (1953), a rectangular hyperbola

$$J_j^{\text{ei}} = V_{\text{jm}}^{\text{app}} \cdot c_j^{\text{e}} / (K_{\text{jm}}^{\text{app}} + c_j^{\text{e}}) \quad (18)$$

was adjusted to these points and was given the meaning of a system of the Michaelis–Menten type (Sect. 3.1). The apparent parameters, V_{jm}^{app} and $1/K_{jm}^{app}$, were assumed to correspond to the maximal inflow (carrier C_j saturated by S_j) and to an approximate value of the affinity of C_j for S_j . With a wide range of c_j^e -values, the distribution of points $\{c_j^e, J_j^{ei}\}$ often had a dual- or multi-phasic aspect, to which it was impossible to adjust a single hyperbola. When two or more hyperbolas could be adjusted to the experimental points, the conventional interpretation was that the transport process involved as many different carriers (C_{j1} , C_{j2} , etc.), the kinetic parameters of which were the apparent parameters (V_{jm1}^{app} and K_{jm1}^{app} , V_{jm2}^{app} and K_{jm2}^{app} , etc.) as calculated from the adjusted hyperbolas (Epstein 1966). When the distribution of experimental points exhibited a sigmoid shape, the carrier was assumed to be an allosteric protein (Glass 1976).

In brief, the conventional formulation aimed to derive precise molecular parameters from the measurement of fluxes into the whole, macroscopic system.

4.2.2 Flow/Force Formulation of Cell Transports

4.2.2.1 Principle of the Flow/Force Formulation

By contrast with the conventional formulation, the Flow/Force formulation aims to determine parameters characteristic of the overall functioning of a transport process, whatever the possible complexity of the underlying molecular mechanisms; i.e. it derives a macroscopic interpretation from the macroscopic flux measurements. Formerly, this approach was termed an “electrokinetic interpretation” because initially inferred from a formal analogy with classical electrokinetics [4–5], but it is in fact [6, 122] a consequence of non-equilibrium thermodynamics (Katchalsky and Curran 1965).

If a plant system (plant roots, water weeds, cell suspension culture, etc.) is left for a long time in a growth solution containing an invariable concentration, ${}^\circ c_j^e$, of a solute S_j , this plant system equilibrates with the external solution. The net flow, J_j , of S_j tends to become equal to zero [$J_j^{ei} = J_j^{ie}$ in (1)] when the growth of the system is negligible, while a non-nil J_j -value simply compensates for the dilution effect due to a non-negligible growth of the system. If larger or smaller values, c_j^e , of the external concentration of S_j are substituted for ${}^\circ c_j^e$, the net flow J_j is changed accordingly. Increasing or decreasing the external concentration can be accomplished by supplying the growth medium with an appropriate quantity of S_j or by diluting it with an appropriate volume of a solution lacking S_j but otherwise identical with the growth solution. According to non-equilibrium thermodynamics, as long as the c_j^e - values are not too different from ${}^\circ c_j^e$, J_j is a linear function of $\ln(c_j^e)$. When all calculations are done [122], this is written

$$J_j = J_j(c_j^e) = R \cdot T \cdot \lambda_j \cdot \ln(c_j^e / {}^\circ c_j^e) = L_j \cdot \ln(c_j^e / {}^\circ c_j^e) \quad (19)$$